TS/LP Note 93-33 (Tech)

14 January 1993

EFFECTS OF SPACE CHARGE IN BUNCHED ELECTRON BEAMS: APPLICATIONS TO THE CLIC TEST FACILITY

A. RICHE
CERN, 1211 Geneva 23, Switzerland

Abstract

The evolution of electron bunches depends on the particle energy, the charge distribution, and the size of the bunches. The interaction with the vacuum chamber, also important, is, however, neglected in this study because it deals with the situation where space-charge effect is dominant. Although there are a number of multiparticle tracking codes, analytical approximations are useful to predict the essential results. Ellipsoidal bunches with different distribution functions, but with identical initial r.m.s. dimensions, are considered. It turns out that evolution of r.m.s. dimensions is quasi-independent of the detailed distribution, and, therefore, the uniform distribution is a good approximation to study the effect of the energy and geometric form factor.

It is possible to separate partially the effects of energy and bunch geometry, which allow one to find scaling laws by using approximations of the forces valid in each interval of variation of the parameters.

In some cases, the equations for the transverse and the longitudinal envelope motion can be resolved analytically. The case of the continuous beam is found as a particular solution. In other cases, the motions are coupled and a step-by-step integration has to be used for a numerical solution. The results are compared with those obtained by the transform of the matrix of the second moments of the beam.

These considerations are applied to the case of the CLIC Test Facility, where a train of bunches of some nC and some ps length, delivered by a 3-GHz RF gun, and accelerated to more than 40 MeV, is used for exciting a 30-GHz CLIC structure.

1 INTRODUCTION

The defocusing effect of space charge is a major difficulty for the creation and the transport of short bunches with high charge. We use as example the CLIC Test Facility [1]. There, the energy of bunches of electrons of some nC charge and some ps length, produced by a 3-GHz RF gun at about 3 MeV/c, is raised to 40 MeV in a 3-GHz accelerating cavity and is then partially absorbed when the bunches excite a travelling-wave structure at 30-GHz, source of high-frequency power. The highest possible charge and a bunch length small compared to the wave length at 30 GHz (1cm) are required. These parameters are strongly influenced by the transverse dimensions, the bunch energy at the gun exit, the energy gain in the acceleration section, and the geometry of the line.
For fixing the parameters and defining the line, it is useful to derive simple analytical formulae for the dynamics from approximations, before performing calculations with more accuracy. The basic hypothesis of the uniform distribution of the charge in an ellipsoidal bunch is justified by the quasi independence of the envelope from the type of the distribution, provided that the initial r.m.s. dimensions are the same in all distributions [2].
Further simplification is obtained from supposing rotational symmetry and from keeping only the most significant part of the expressions of the self force, valid in limited intervals of variation of the energy and of the bunch geometry.
With these approximations, it is possible to formulate the scaling laws for the variation of the self force, hence of the dynamics, with the geometry of the bunch and with the energy, because their effects can be partially separated. In this case also, and supposing that the beam is laminar, the equation of the envelope can be solved analytically for bunches which are very long (the limiting case is the continuous beam), or very short in their rest frame. These solutions, illustrated by examples, are compared for verification with those given by using TRANSPORT [3] complemented by a subroutine which takes into account the space-charge forces. The use of the beam matrix is justified for a uniform distribution. Examples are given for the configuration for the CTF experiment.

2 FORCE DUE TO THE SPACE CHARGE

The force applied on an electron of a bunch is evaluated in free space. The distribution of the charge is supposed to be constant on the surface of similar ellipsoids. To simplify the writing, we take the example of the ellipsoidal bunch with rotational symmetry, which has an axis in the direction of propagation. The components for the force are calculated in the rest system of the bunch, where the fields are electrostatic. The components in the laboratory frame are derived from those in the rest system, and introduced in the equation for the dynamics.

2.1 Potentials for Space-Unlimited and -Limited Distributions

Consider an unlimited elliptical distribution $n(u)$ of r.m.s. size a_R in the radial direction and b_R in the longitudinal direction: $u = r^2/a_R^2 + z^2/b_R^2$. A simple example would be the Gaussian: $n(u) = \exp(-u/2)$. The potential of the electrostatic field can be written as [4]

$$\phi = -\frac{e\, a_R^2\, b_R}{4\, \epsilon_0} \int_0^\infty \frac{g(U)}{v(s)} \mathrm{d}s$$

where:

$$U = \frac{r^2}{a_R^2 + s} + \frac{z^2}{b_R^2 + s}$$

$$\frac{\mathrm{d}g}{\mathrm{d}s} = n(U)$$

$$v(s) = \left(\left(a_R^2 + s\right)^2 \left(b_R^2 + s\right)\right)^{1/2} .$$

Verifying that the potential satisfies Poisson's equation is easy when noting that:

$$\nabla\, g(U) = -4\, \frac{\partial}{\partial s} \frac{n(U)}{v(s)} .$$

The radial electric field component, taken as example is:

$$E_r = \frac{a_R^2\, b_R}{2\, \epsilon_0}\, r \int_0^\infty \frac{n(U)}{v(s)} \mathrm{d}s .$$

By $n(U)$, r and z appear in the integral, thus the field is not linear. However, the envelope motion is very similar to the envelope motion of an equivalent uniform distribution with the same initial r.m.s. size [2].

Consider a bunch of charges uniformly distributed in an ellipsoid of half axis a_R and b_R. The potential can be written as [5]:

$$\phi = \frac{e}{4\, \epsilon_0}\, a_R^2\, b_R\, n \int_\xi^\infty \frac{1 - U}{v} \mathrm{d}s .$$

The distribution n is constant in the ellipsoid.

For a point external to the ellipsoid, ξ is given by:

$$\frac{r^2}{a^2 + \xi} + \frac{z^2}{b^2 + \xi} = 1 .$$

For a point situated in the ellipsoid, ξ is null. Both potentials satisfy Poisson's equation and the fields are continuous at the limit of the distribution. The components of the field are, for a point in the ellipsoid:

$$E_r = \frac{e}{2\, \epsilon_0}\, a_R^2\, b_R\, n\, r \int_0^\infty \left(a_R^2 + s\right)^{-1} \left(\left(a_R^2 + s\right)^2 \left(b_R^2 + s\right)\right)^{-1/2} \mathrm{d}s$$

$$E_z = \frac{e}{2\, \epsilon_0}\, a_R^2\, b_R\, n\, r \int_0^\infty \left(b_R^2 + s\right)^{-1} \left(\left(a_R^2 + s\right)^2 \left(b_R^2 + s\right)\right)^{-1/2} \mathrm{d}s . \qquad (1)$$

They vary linearly with the corresponding coordinate. For a three-dimensional ellipsoidal bunch, elliptic integrals should be used. With the assumed rotational symmetry, integration gives:

$$E_r = \frac{e}{2\, \epsilon_0}\, n\, r\, I_r^R$$

$$E_z = \frac{e}{2\, \epsilon_0}\, n\, z\, I_z^R \qquad (2)$$

with:

$$I_r^R = 1 - J\ , \quad I_z^R = 2\, J$$

for $x < 1$,

$$J = \frac{x^2}{(1-x^2)^{3/2}} \left(\frac{1+(1-x^2)^{1/2}}{x} - 1 \right)$$

for $x \geq 1$,

$$J = \frac{x^2}{(x^2-1)^{1/2}} \left(1 - \frac{\arctan (x^2-1)^{1/2}}{(x^2-1)^{1/2}} \right) \tag{3}$$

2.2 Forces in the Rest Frame and in the Laboratory Frame

In the rest frame, the fields are purely electrostatic. With the expressions of the fields given in Eq. (1) for the uniform distribution, the components at a point (r_R, z_R) within the ellipsoid in the rest frame are:

$$f_r^R = \frac{3\ e\ Q}{8\ \pi\ \epsilon_0} \frac{I_r^R}{a_R^2\ b_R}\ r_R$$

$$f_z^R = \frac{3\ e\ Q}{8\ \pi\ \epsilon_0} \frac{I_z^R}{a_R^2\ b_R}\ z_R\ . \tag{4}$$

All geometric lengths are given in the rest frame. The components r and z of the position in the laboratory frame are: $r = r_R$, $z = z_R/\gamma$; and the radial size and longitudinal half axis of the ellipsoid: $a = a_R$, $b = b_R/\gamma$. The components of the force in the laboratory frame are given by the Lorentz transform of the forces: $f_r = \gamma^{-1} f_r^R$; $f_z = f_z^R$. With all the lengths measured in the laboratory frame, the components are:

$$f_r = \frac{3\ e\ Q}{8\ \pi\ \epsilon_0} \frac{I_r(x)}{a^2\ b\ \gamma^2}\ r$$

$$f_z = \frac{3\ e\ Q}{8\ \pi\ \epsilon_0} \frac{I_z(x)}{a^2\ b}\ z\ . \tag{5}$$

Q is the charge, invariant in the transformation, and I_r and I_z are functions of γ through:

$$x = a/(\gamma\ b)\ .$$

3 MOTION IN THE LABORATORY FRAME

In order to find approximate envelope equations for the space-charge dominated motion of a bunch along a short longitudinal path, as in transfer lines or linacs, the following pairs of variables are used:

$$r,\ \mathrm{d}r/\mathrm{d}s,\ z,\ \Delta p/p\ .$$

The trajectory of a particle is referenced to the trajectory of the central particle of the bunch: r and z are the transverse and the longitudinal distances from the central particle; s, v and p are the length of the path, the speed and the momentum for the particle at the centre of the bunch; $\vec{\Delta p}$ is the difference in momentum, with the components:

$$\Delta p_r = m\ \gamma\ v\ \frac{\mathrm{d}r}{\mathrm{d}s}$$

$$\Delta p_z = m\ \gamma\ v\ \frac{\Delta p}{p}\ .$$

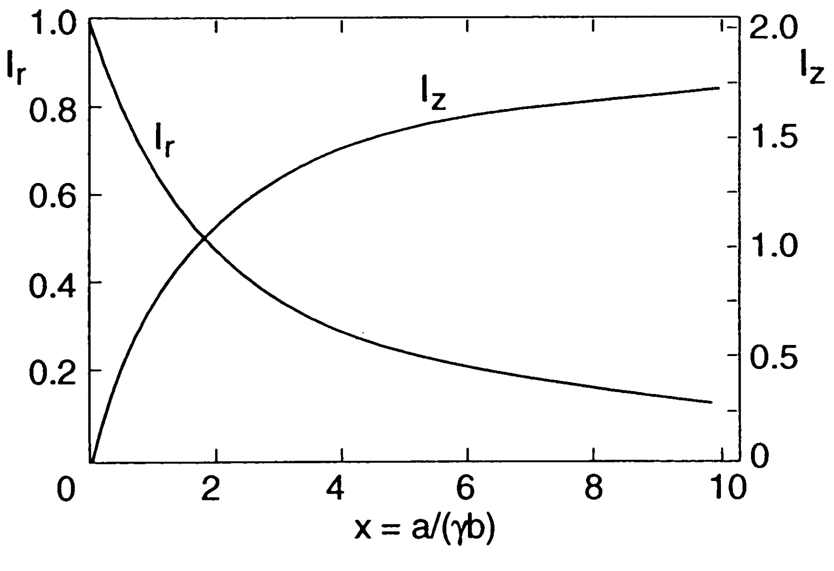

Figure 1: Space charge integrals I_r,I_z, as a function of $x = a/(\gamma b)$

Applying Newton's law to the particle and to the particle at the centre, we have by difference:

$$v \frac{\mathrm{d}}{\mathrm{d}s}\Delta\vec{p} = \vec{f} \; . \tag{6}$$

By projection:

$$\frac{\mathrm{d}^2 r}{\mathrm{d}s^2} = -\frac{\gamma}{\gamma^2 - 1} \frac{\mathrm{d}\gamma}{\mathrm{d}s}\frac{\mathrm{d}r}{\mathrm{d}s} + \frac{1}{m\gamma v^2} f_r$$

$$\frac{\mathrm{d}}{\mathrm{d}s}\frac{\Delta p}{p} = -\frac{\gamma}{\gamma^2 - 1} \frac{\mathrm{d}\gamma}{\mathrm{d}s}\frac{\Delta p}{p} + \frac{1}{m\gamma v^2} f_z \; . \tag{7}$$

In the absence of external fields, γ is constant. Substituting the components of the force, we have:

$$\frac{\mathrm{d}^2 r}{\mathrm{d}s^2} = \frac{3 \; e \; Q}{8 \; \pi \; \epsilon_0 \; mc^2} \; \frac{I_r(x)}{a^2 \; b \; \beta^2 \; \gamma^3} \; r \tag{8}$$

$$\frac{\mathrm{d}}{\mathrm{d}s}\frac{\Delta p}{p} = \frac{3 \; e \; Q}{8 \; \pi \; \epsilon_0 \; mc^2} \; \frac{I_z(x)}{a^2 \; b \; \beta^2 \; \gamma} \; z \; . \tag{9}$$

4 SCALING LAWS FOR THE FORCES AND THEIR EFFECTS

According to Eqs. (5), the force is proportional to the charge density $Q/(4\ \pi/3\ a^2 b)$ in the bunch. The component f_r is a function of γ^2 and of $a/(\gamma b)$, by I_r; the component f_z, a function of $a/(\gamma b)$ by I_z. The effects of γ and of the form factor a/b cannot be separated. However, when considering each of the different intervals of $x = a/(\gamma b)$, there is an approximation for I_r and for I_z which separates the effect of γ from the effect of a/b. This approximation is necessarily of the form:

$$I = k \;\; x^n \; .$$

The values of k and n in each interval are determined by comparing $I = k\ x^n$ with the exact variation of I_r and I_z with x, as represented in Fig. 1. Thus, Fig. 2 gives n and k for I_r as a continuous function of x. In Table 1, the same result is obtained from comparing $I = k\ x^n$ with the approximations of I_r and I_z in three regions: $x \to 0$, $x \to \infty$, $x \sim 1$.

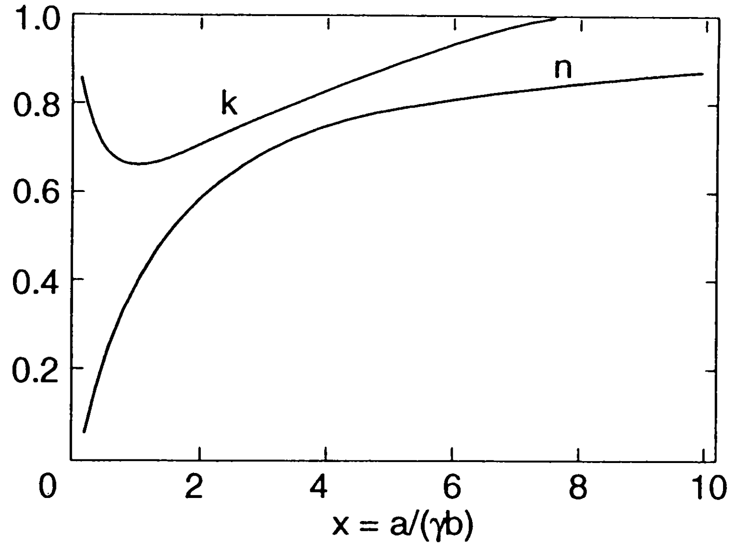

Figure 2: Approximation of the space charge Integral I_r by $I_r = kx^{-n}$: Values of n and of k as functions of $x = a/(\gamma b)$

TABLE 1: Space-charge integral asymptotic values and intermediate approximation.

$x = a/(\gamma b)$	0	1	∞
I_r^R	$1 - 0.15 \times 10^2\ x^2$ k_r	$1 - 0.4\ x$ k_r	$\pi\,(2\ x)^{-1}$ $k_r\ x^{-1}$
I_z^R	$0.3 \times 10^2\ x^2$ $k_z\ x^2$	$0.8\ x$ $k_z\ x$	$2\left(1 - \pi\ (2\ x)^{-1}\right)$ k_z

4.1 Forces

The components of the force in Eq. (5) are proportional to the charge density and to the simple functions of γ and a/b introduced with the approximations on the space-charge integrals. The substitution gives:

– Low energy: $\gamma \ll a/b$

$$f_r = \frac{3\ e\ Q}{8\ \pi\ \epsilon_0\ a^2\ b}\ \frac{\pi\ b\ r}{2\ a\ \gamma} \tag{10}$$

$$f_z = \frac{3\ e\ Q}{8\ \pi\ \epsilon_0\ a^2\ b}\ 2\left(1 - \frac{\pi\ \gamma\ b}{2\ a}\right)\ z \tag{11}$$

– Medium energy: $\gamma \sim a/b$

$$f_r = \frac{3\ e\ Q}{8\ \pi\ \epsilon_0\ a^2\ b}\left(1 - 0.4\frac{a}{\gamma\ b}\right)\ \frac{r}{\gamma^2} \tag{12}$$

$$f_z = \frac{3\ e\ Q}{8\ \pi\ \epsilon_0\ a^2\ b}\ \frac{0.8\ a}{b}\ \frac{z}{\gamma} \tag{13}$$

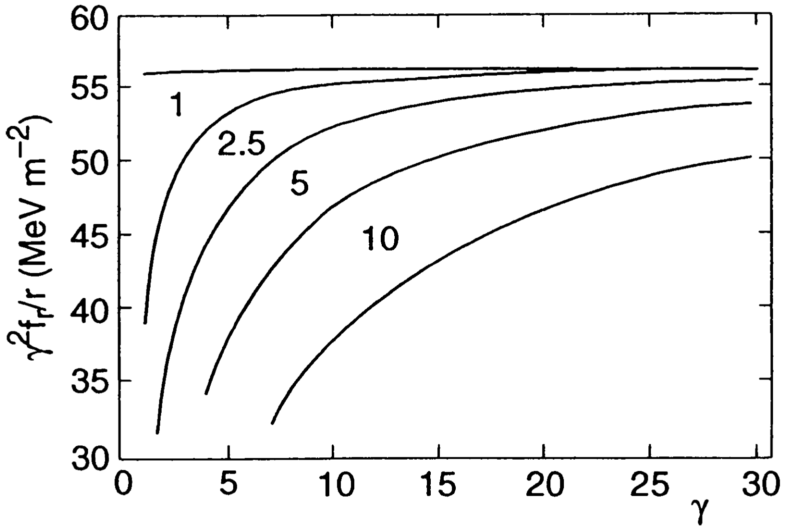

Figure 3: Transverse force, multiplied by γ^2, scaled in MeV m^{-2} , per unit radial distance r to bunch centre, for a bunch of 1 nC in 1 m^3. The aspect ratio a/b is the parameter on the curves

– High energy: $\gamma \gg a/b$

$$f_r = \frac{3\ e\ Q}{8\ \pi\ \epsilon_0\ a^2\ b}\ \frac{r}{\gamma^2} \tag{14}$$

$$f_z = \frac{3\ e\ Q}{8\ \pi\ \epsilon_0\ a^2\ b}\ 0.3\ 10^2 \left(\frac{a}{b}\right)^2 \frac{z}{\gamma^2} \tag{15}$$

4.2 Acceleration

The beam dynamics equations are derived by substituting the components of the force in the expressions (7) giving $\mathrm{d}^2 r/\mathrm{d}s^2$ and $\mathrm{d}/\mathrm{d}s\,(\Delta p/p)$. For constant energy, we have:

$$\frac{\mathrm{d}^2 r}{\mathrm{d}s^2} = \frac{1}{mc^2}\ \frac{1}{\beta^2\gamma}\ f_r \tag{16}$$

$$\frac{\mathrm{d}}{\mathrm{d}s}\frac{\Delta p}{p} = \frac{1}{mc^2}\ \frac{1}{\beta^2\gamma}\ f_z\ . \tag{17}$$

By derivation of $\gamma\beta$, one obtains the classical formula:

$$\frac{\Delta p}{p} = \gamma^2\ \frac{\mathrm{d}z}{\mathrm{d}s}\ , \tag{18}$$

so that, at constant energy, the expression of $\mathrm{d}^2 z/\mathrm{d}s^2$ is:

$$\frac{\mathrm{d}^2 z}{\mathrm{d}s^2} = \frac{1}{\gamma^2}\ \frac{\mathrm{d}}{\mathrm{d}s}\frac{\Delta p}{p}\ . \tag{19}$$

4.3 Scaling Laws

– The scaling laws for the variation with γ of the components of the force, and of the acceleration are summarized in Table 2.
  The components of the force calculated in the laboratory frame are represented in graphs. The results are given for a charge of 1 nC distributed in 1 m^3.

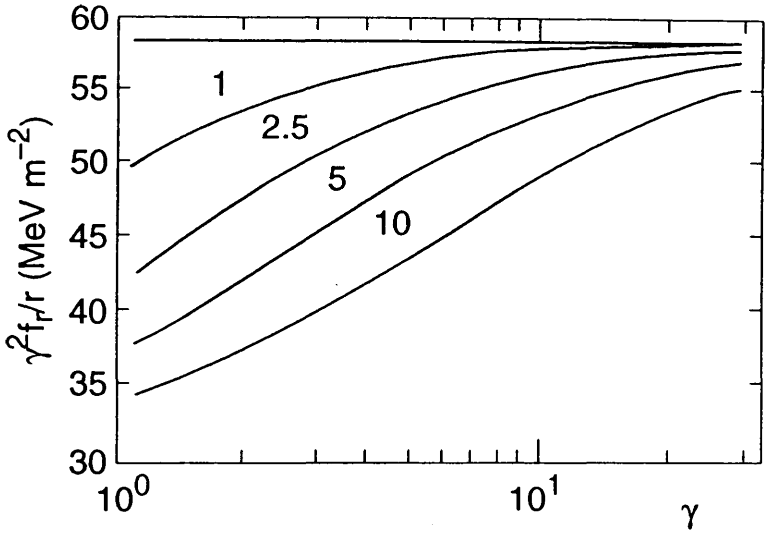

Figure 4: Transverse force, same as Fig. 3, but with a logarithmic scale for γ on the horizontal axis

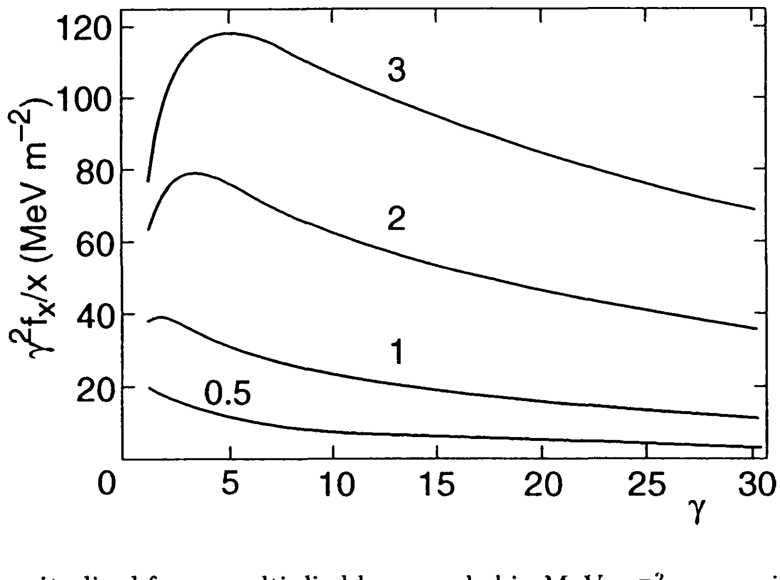

Figure 5: Longitudinal force, multiplied by γ, scaled in MeV m^{-2} , per unit longitudinal distance z to bunch centre, for a bunch of 1 nC in 1 m^3. The aspect ratio a/b is the parameter on the curves

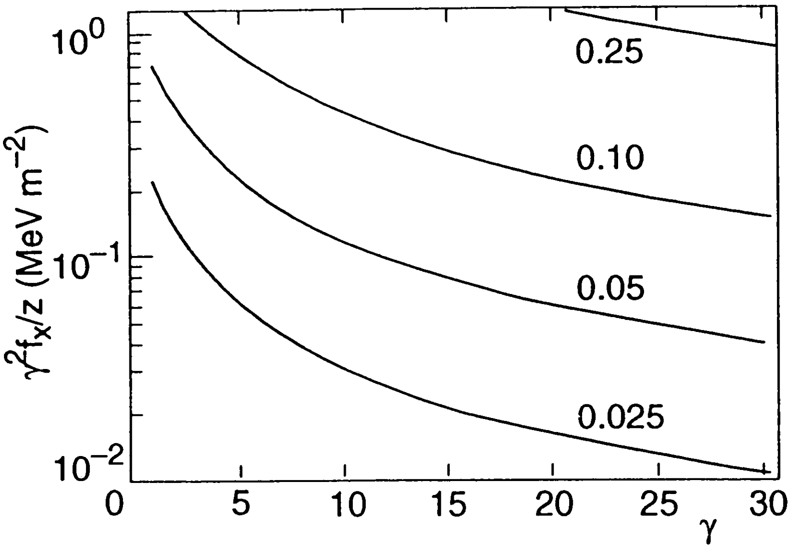

Figure 6: Longitudinal force, same as Fig. 5, but with a logarithmic scale for $\gamma F_z/z$ on the vertical axis

- Radial force
  $\gamma^2\ f_r/r$ in MeV m^{-2}, functions of γ and a/b (Fig. 3)
  the same functions, but with a logarithmic scale for γ for readability (Fig. 4)
- Longitudinal force
  $\gamma\ f_z/z$ in MeV m^{-2}, functions of γ and a/b (Fig. 5)
  the same functions, but with a logarithmic scale for the functions (Fig. 6)

The corresponding values of acceleration $\mathrm{d}^2 r/\mathrm{d}s^2$ and $\mathrm{d}/\mathrm{d}s(\Delta p/p)$ are obtained by division by $mc^2\ \beta^2\ \gamma$.

TABLE 2: Scaling with γ of the force, acceleration and dispersion derivative.

Energy	Low	Medium	High
	$\gamma \ll a/b$	$\gamma \sim a/b$	$\gamma \gg a/b$
Radial force	$1/\gamma$	$1/\gamma^n,\ 1<n<2$	$1/\gamma^2$
Longit. force	constant	$1/\gamma^m,\ 0<m<2$	$1/\gamma^2$
$\mathrm{d}^2 r/\mathrm{d}s^2$	$1/(\gamma^2\beta^2)$	$1/(\gamma^{n+1}\beta^2),\ 1<n<2$	$1/(\gamma^3\beta^2)$
$\mathrm{d}(\Delta p/p)/\mathrm{d}s$	$1/(\gamma\beta^2)$	$1/(\gamma^{m+1}\beta^2),\ 0<m<2$	$1/(\gamma^3\beta^2)$
$\mathrm{d}^2 z/\mathrm{d}s^2$	$1/(\gamma^3\beta^2)$	$1/(\gamma^{m+3}\beta^2),\ 0<m<2$	$1/(\gamma^5\beta^2)$

5 COMPARISON WITH DC BEAMS

The force and the acceleration for d.c. beams can be derived from those established for bunch beams by letting the bunch length tend to infinity. As $\gamma \gg a/b$, we are then in the high-energy case. The relation between the volume density ρ of the charge, the current I and the speed v of the electrons is: $I = \pi\ a^2\ \rho\ v$. Expressing the charge Q as a function of the current I in Eq. (14) and Eq. (15) gives the expressions known for continuous beams:

$$f_r = \frac{e\ I\ r}{2\ \pi\ \epsilon_0\ a^2\ v\ \gamma^2}\ . \tag{20}$$

The equation of motion, at constant energy is [6],[7]:

$$\frac{\mathrm{d}^2 r}{\mathrm{d}s^2} = \frac{e}{2\,\pi\,\epsilon_0\,mc^3}\,\frac{I\,r}{a^2\gamma^3\beta^3}\;. \tag{21}$$

6 ENVELOPE MOTION IN DRIFT SPACE

In a laminar flow, the trajectory of the particle at the edge of the bunch defines the bunch envelope. The envelope equations are given by setting $r = a$ and $z = b$ in Eqs. (16), (17) and (19) where f_r and f_z are substituted according to their approximated expressions in section 4.1.

6.1 Low Energy: $\gamma \ll a/b$

With f_r and f_z given by Eqs. (10) and (11), the envelope equations are:

$$\frac{\mathrm{d}^2 r}{\mathrm{d}s^2} = \frac{3\,e\,Q}{16\,\epsilon_0\,mc^2}\,\frac{1}{\gamma^2\,\beta^2\,r^2} \tag{22}$$

$$\frac{\mathrm{d}^2 z}{\mathrm{d}s^2} = \frac{3\,e\,Q}{4\,\pi\,\epsilon_0\,mc^2}\,\frac{1}{\gamma^3\,\beta^2\,r^2}\left(1-\frac{\pi\,\gamma\,z}{2\,r}\right)\;. \tag{23}$$

Since the equation for the radial motion does not contain z, one can use the following reduced variables:

$$R = \frac{r}{r_0}\quad , \quad \text{and} \quad S = \left(\frac{3\,e\,Q}{8\,\epsilon_0\,mc^2}\frac{1}{r_0}\right)^{1/2}\frac{s}{\gamma\,\beta\,r_0}\;. \tag{24}$$

The solution of Eq. (22) is then:

$$\frac{\mathrm{d}R}{\mathrm{d}S} = \mathrm{sign}\left(\frac{\mathrm{d}R}{\mathrm{d}S}\right)_0\left(\left(\frac{\mathrm{d}R}{\mathrm{d}S}\right)_0^2 + 1 - \frac{1}{R}\right)^{1/2}\;. \tag{25}$$

For a negative value of $(\mathrm{d}R/\mathrm{d}S)_0$, the motion begins with a decreasing radius $R(S)$ and with increasing $\mathrm{d}R/\mathrm{d}S$ due to the force. The derivative of R passes by 0 for $R = R_m$:

$$R_m = \left(1 + \left(\frac{\mathrm{d}R}{\mathrm{d}S}\right)_0^2\right)^{-1} \tag{26}$$

and then reaches the positive value $-\,(\mathrm{d}R/\mathrm{d}S)_0$ for which R is again equal to $R_0 = 1$ in Eq. (25). The envelope is therefore symmetric with the position S_m for which the minimum R_m for R is found. Integrating Eq. (25) gives the longitudinal azimuth S as a function of the radius R:

$$S = S_0 + \mathrm{sign}\,\left(\frac{\mathrm{d}R}{\mathrm{d}S}\right)_0\Big(T(R) - T(R_0 = 1)\Big)$$

where

$$T = \frac{R_m^{3/2}}{2}\left(\log\left|\frac{(1/R_m - 1/R)^{1/2} + 1/R_m^{1/2}}{(1/R_m - 1/R)^{1/2} - 1/R_m^{1/2}}\right| + \frac{2R}{R_m^{1/2}}(1/R_m - 1/R)^{1/2}\right)\;. \tag{27}$$

For $R = R_m$, we have $S_m = S_0 + T(1)$, function of R_m. This function has a maximum:

$$S_M \sim 0.835\;\; \text{for}\; R_M \sim 0.612;\quad \text{or}\;\; (\mathrm{d}R/\mathrm{d}S)_{0M} \sim -0.796\;.$$

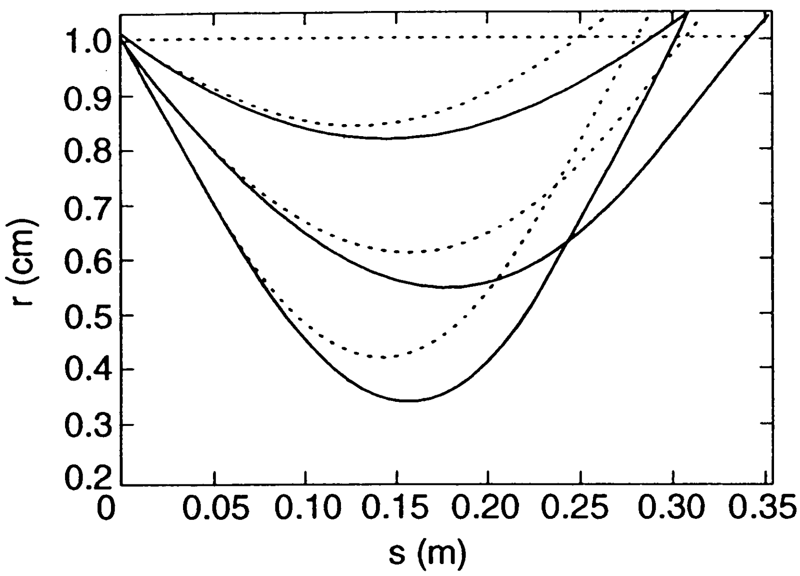

Figure 7: Envelopes for transverse motion for a bunch with $\gamma = 6$ (low energy). $a = 10$ mm, $b = 0.166$ mm, $Q = 12.6$ nC, $a/(b\gamma) = 10$, for three values of the initial angle $\mathrm{d}r/\mathrm{d}s$. The intermediate value of $\mathrm{d}r/\mathrm{d}s$ corresponds to the maximum length for transmitting the charge with $r < a$. The analytical approximation (dotted line) is compared with the calculations by matrices (continuous line)

For a given value of Q, the value of S_M substituted in Eq. (24) gives a maximum range $s = 2\ s_M$ for which $r \leq r_0$, while for a given value of s, it gives a maximum Q_M for the charge which can be transmitted along 2 s without loss ($r \leq r_0$).

$$Q_M = \frac{8\ mc^2\ \epsilon_0}{3\ e} S_M^2 (\gamma\beta)^2 r_0 \left(\frac{r_0}{s}\right)^2 . \tag{28}$$

Since, in reduced coordinates:

$$(\mathrm{d}R/\mathrm{d}S)_{0\ M}\ S_M = -0.66$$

in the original coordinates:

$$(\mathrm{d}r/\mathrm{d}s)_{0\ M} = -0.66\ r_0/s_M.$$

When the conditions for a maximum S_M are fulfilled, the tangent to the envelope at the initial point crosses the axis at a distance $1.33\ s_M$. If the initial angle is provided by a focusing device, the focal length required for the optimum solution is $f = 1.33\ s_M$.

Figure 7 represents the envelopes for the transverse motion according to the preceding approximations. The bunch is short: the aspect ratio is 60 in the laboratory frame and 10 in the rest frame of the bunch for $\gamma = 6$. To test the accuracy of the analytical solution, the envelopes are compared with those derived from the matrix formalism.

Once the envelope is known for the transverse motion, the solution for the longitudinal motion follows because of the similarity between Eqs. (22) and (23). The motion for z may be deduced from the motion for r by:

$$z = z_0 + s\left(\left(\frac{\mathrm{d}z}{\mathrm{d}s}\right)_0 - \frac{4}{\pi\ \gamma}\left(\frac{\mathrm{d}r}{\mathrm{d}s}\right)_0\right) + \frac{4}{\pi\ \gamma}(r - r_0) .$$

6.2 Medium Energy: $\gamma \sim a/b$

The equations for the motion are approximately

$$\frac{\mathrm{d}^2 r}{\mathrm{d}s^2} = \frac{3\ e\ Q}{8\ \pi\ \epsilon_0\ mc^2}\ \frac{1}{r\ z\ \gamma^3\ \beta^2} \tag{29}$$

$$\frac{\mathrm{d}^2 z}{\mathrm{d}s^2} = \frac{3\ e\ Q}{8\ \pi\ \epsilon_0\ mc^2}\ \frac{0.8}{r\ z\ \gamma^4\ \beta^2}\ . \tag{30}$$

The transverse and the longitudinal motion are coupled. A step-by-step numerical integration should be used to solve the system of differential equations.

6.3 High Energy: $\gamma \gg a/b$

The envelope equations are obtained from Eqs. (16), (17) with the approximations (14),(15) for the space-charge integrals at high energy:

$$\frac{\mathrm{d}^2 r}{\mathrm{d}s^2} = \frac{3\ e\ Q}{8\ \pi\ \epsilon_0\ mc^2}\ \frac{1}{r\ z\ \gamma^3\ \beta^2} \tag{31}$$

$$\frac{\mathrm{d}^2 z}{\mathrm{d}s^2} = \frac{10^2\ e\ Q}{8\ \pi\ \epsilon_0\ mc^2}\ \frac{1}{z^2\ \gamma^5\ \beta^2}\ . \tag{32}$$

Equation (32) for the longitudinal motion is similar to Eq. (22) for the radial motion for the low-energy case: the solution and the discussion are similar. However, the ratio between the constant factors in the r.h.s. of Eqs. (32) and (22) is approximately $\sim 4/\gamma^3$.

For high γ and long bunch length, the change in $\mathrm{d}z/\mathrm{d}s$ may be neglected when considering the radial motion. If the initial value for $\mathrm{d}z/\mathrm{d}s$ is small, the variation of z can be neglected in Eq. (31). With $z = b$ constant, the Eq. (31) for radial motion is the equation usually discussed for space-charge effects in d.c. beams.

We follow a beam which is convergent at the initial position, and for which the energy and initial sizes are such that $(r/b\ \gamma)_0 \ll 1$. The radial size goes to a minimum, then increases because of the action of the space charge.

We have to repeat a formalism similar to the one used for low energy, because the expressions are different. Changing for reduced variables,

$$R = \frac{r}{r_0}\quad ,\quad \text{and}\quad S = \left(\frac{3\ e\ Q}{4\ \pi\ \epsilon_0\ mc^2}\frac{1}{\gamma\ b}\right)^{1/2}\ \frac{s}{\beta\ \gamma\ r_0} \tag{33}$$

we obtain:

$$\frac{\mathrm{d}^2 R}{\mathrm{d}S^2} = \frac{1}{2R}$$

with the solution

$$(\mathrm{d}R/\mathrm{d}S) = \mathrm{sign}(\mathrm{d}R/\mathrm{d}S)_0\ \left(\log R + (\mathrm{dR/dS})_0^2\right)^{1/2}\ . \tag{34}$$

Integrating over $R' = \mathrm{d}R/\mathrm{d}S$, we get:

$$S = \exp\left(-{R_0'}^2/2\right) \int_{R_0'}^{R'} \exp\left(+R'^2/2\right)\ \mathrm{d}R'\ . \tag{35}$$

Let S_m be the value of S obtained from Eq. (35), between the points at which $R' = R_0'$ (origin) and the points at which $R' = 0$ (minimum radius of the envelope). The integration gives a result identical to S_m if the limits are $R' = 0$ and $R' = -R'_0$. Therefore the envelope is symmetric with the position S_m for which the minimum R_m of R is found.

Let R'_0 vary. There is a maximum S_M for S_m, found for $\mathrm{d}S_m/\mathrm{d}R'_0 = 0$, i.e. for:

$$R'_0 \int_{R'_0}^{0} \exp\left(-R'^2/2\right)\ \mathrm{d}R' + \exp\left({R'_0}^2/2\right) = 0 \ .$$

The solution $R'_{0\ M}$ is: $R'_{0\ M} \sim -0.92$;
S_M is given by Eq. (35) for $R'_0 = R'_{0\ M}$ and $R' = 0$: $S_m \sim 1.08$.
The maximum range for which $R \leq R_0$ is: $S = 2\ S_M \sim 2.16$. For $\mathrm{d}R/\mathrm{d}S = 0$, Eq. (34) gives: $R_m \sim \exp -{R'_0}^2$ and, for $R'_{0\ M} = -0.92$ (maximum range S_M), R_m takes the value R_M : $R_M = r_M/r_0 \sim 0.43$.
For a given value of Q, the value of S_M substituted in Eq. (33), gives a maximum range $s = 2\ s_M$ for which $r \leq r_0$, while for a given value of s, it gives a maximum Q_M for the charge which can be transmitted along $2\ s$ without loss ($r \leq r_0$).

$$Q_M = \frac{4\ \pi\ mc^2\ \epsilon_0}{3\ e}\ b\ S_M^2 \gamma^3 \beta^2\ (\frac{r_0}{s})^2 \ . \qquad (36)$$

Since, in reduced coordinates:

$$(\mathrm{d}R/\mathrm{d}S)_{0\ M}\ \ S_M = -1.0 \ ,$$

in the original coordinates:

$$(\mathrm{d}r/\mathrm{d}s)_{0\ M} = -r_0/s_M \ .$$

When the conditions for a maximum S_M are fulfilled, the tangent to the envelope at the initial point crosses the axis at a distance s_M. If the initial angle is provided by a focusing device, the focal length should be $f = s_M$.

Figure 8 represents the envelopes for the transverse motion for a bunch with an aspect ratio of 0.83 in the laboratory frame, and, for $\gamma = 7.5$, a corresponding aspect ratio of 0.11 in the rest frame. To test the accuracy of the analytical solution, these envelopes are compared with those obtained from the matrix formalism.
The solutions for the radial motion in the case $a/(b\ \gamma) \ll 1$ are the same as the solutions for the cylindrical continuous beam. For a discussion about a two-dimensional continuous cylindrical beam, we refer to Pierce [6] and to Baconnier and Pisent [7].

7 ENVELOPE MOTION IN ACCELERATING STRUCTURES

The external accelerating force is identical for all the electrons of the bunch. Supposing an axial electric field E, it modifies the axial momentum by:

$$\frac{\mathrm{d}(\beta\ \gamma)}{\mathrm{d}s} = \frac{e\ E}{mc^2\ \beta} \ .$$

The differential equation for the radial motion is given in Eq.(7):

$$\frac{\mathrm{d}^2 r}{\mathrm{d}s^2} = -\frac{\gamma}{\gamma^2 - 1}\ \frac{\mathrm{d}\gamma}{\mathrm{d}s}\ \frac{\mathrm{d}r}{\mathrm{d}s} + \frac{1}{mc^2 \gamma\ \beta^2}\ f_r \ .$$

For the example, we take the high energy approximation $\gamma \gg a/b$. According to Eq. (14)

$$f_r = \frac{3\ e\ Q}{8\ \pi\ \epsilon_0}\ \frac{r}{a^2\ b\ \gamma^2} \ .$$

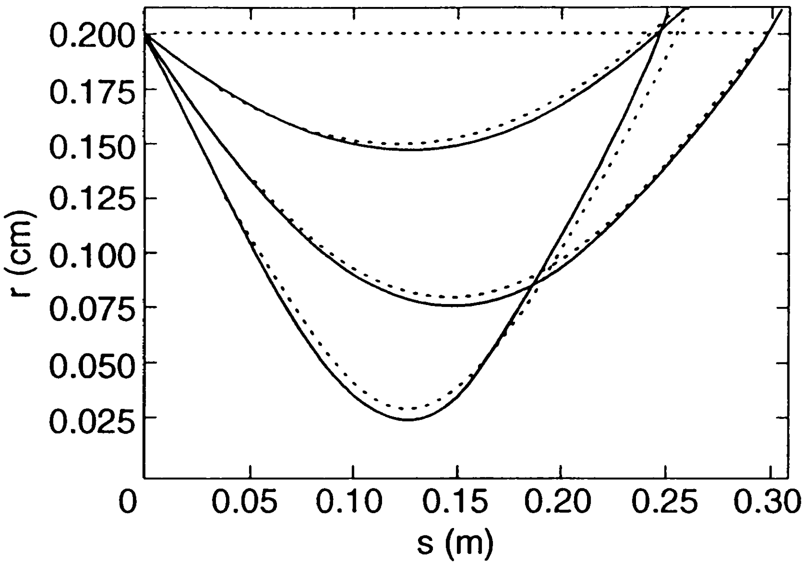

Figure 8: Envelopes for transverse motion for a bunch with $\gamma = 7.5$ (high energy). $a = 2$ mm, $b = 2.4$ mm, $Q = 4.2$ nC, $a/(b\gamma) = 0.1$, for three values of the initial angle $\mathrm{d}r/\mathrm{d}s$. The intermediate value of $\mathrm{d}r/\mathrm{d}s$ corresponds to the maximum length for transmitting the charge with $r < a$. The analytical approximation (dotted line) is compared with the calculations by matrices (continuous line)

If the particle is at the edge of the bunch, $r = a$, $z = b$. The envelope equation is the same equation as for a drift, but we now have a term proportional to dr/ds:

$$\frac{\mathrm{d}^2 r}{\mathrm{d}s^2} = -\frac{e\,E}{mc^2\,\beta^2\,\gamma}\,\frac{\mathrm{d}r}{\mathrm{d}s} + \frac{3\,e\,Q}{8\,\pi\,\epsilon_0\,mc^2}\,\frac{1}{r\,z\,\gamma^3\,\beta^2}\;.$$

The variation of z is neglected as in the case without acceleration. It is possible to find reduced variables when the electric field E is independent of s. The new variable is γ:

$$\frac{\mathrm{d}\gamma}{\mathrm{d}s} = \frac{e\,E}{mc^2}\;.$$

The new function R is defined by:

$$R = \frac{e\,E}{mc^2}\left(\frac{3\,e\,Q}{8\,\pi\,\epsilon_0\,mc^2\,b}\right)^{-1/2} r$$

With these variables, the equation of the envelope is:

$$\left(1 - \frac{1}{\gamma^2}\right)\gamma\,\frac{\mathrm{d}^2 R}{\mathrm{d}\gamma^2} + \frac{\mathrm{d}R}{\mathrm{d}\gamma} = \frac{1}{\gamma^2}\frac{1}{R}\;.$$

When γ is high, the r.h.s. term of the equation tends to 0. In this case, a simple integration gives the result known for the travelling-wave accelerator for a particle in phase with the maximum field (no space-charge force):

$$R - R_0 = \frac{mc^2}{e\,E}\left(\gamma_0^2 - 1\right)^{1/2}(\mathrm{d}R/\mathrm{d}s)_0\,\log\frac{\gamma + \left(\gamma^2 - 1\right)^{1/2}}{\gamma_0 + \left(\gamma_0^2 - 1\right)^{1/2}}\;.$$

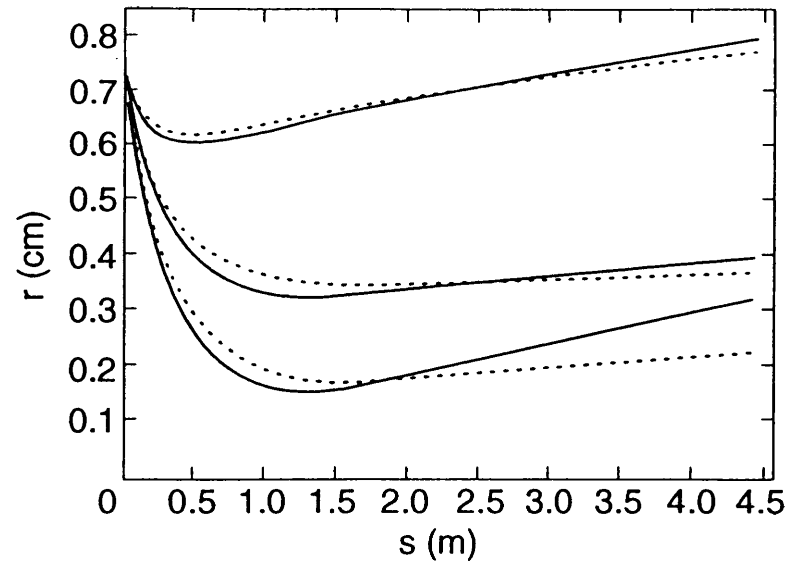

Figure 9: Envelopes for transverse motion in an accelerating structure, for $\gamma_0 = 6$; $a = 7.2$ mm, $b = 4$ mm, $Q = 9.4$ nC, longitudinal electric field 10 MV/m, from $s = 0$ onward. The envelopes are plotted for three values of the initial angle. The approximate solution (dotted line) is compared with the calculations by matrices (continuous lines)

The envelope for the motion with space charge is obtained by numerical integration. On Fig. 9 the envelopes are represented for an aspect ratio of the bunch which is 1.8 at the entrance of a 10 MV/m accelerating section. Accuracy is tested by comparing with the envelopes obtained from the matrix formalism. Very similar results, not represented, are obtained by integrating the complete differential system, with the same approximated value for the radial force, but an axial force different from zero.

8 MATRIX SOLUTION

Generally, the size of the bunch varies in all directions and the differential equation for one projected motion depends also on the size of the bunch in the other projections. Results obtained with the simple approximations of the preceding sections should be compared with those obtained by tracking the individual particles in parallel. But if the external forces are linear with the coordinates, and the internal forces also, as for the uniform distribution, the collective motion of the bunch can then be obtained from the transform of the matrix of the second moments of the distribution.

If the distribution is not uniform, the calculation made with the uniform distribution with the same r.m.s. values gives a good approximation for the envelopes. Several programs [8–13] have been developed, using the results established by Sacherer [2] and Lapostolle [14], [15] for linear forces.

By evaluating the effects of the space charge resulting from each step ds in s in the thin-lens approximation and applying them only at the end of the interval ds, the self-force effect is separated from the effect of the other forces. In this case, the implementation of an existing program, TRANSPORT [3], is possible with a single routine which, for each element, sets the matrix for the action of the charge. However, the elements of the beam line should be short or partitioned for the sake of precision. In the case of an ellipsoidal bunch which has one axis in the direction of motion, the product of the two matrices

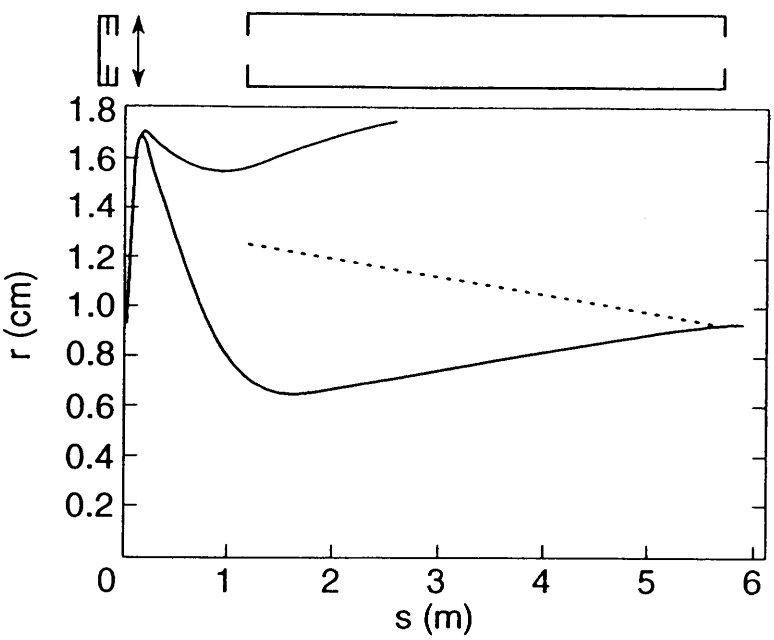

Figure 10: Transverse envelope for a CTF scheme with a 3.9-MeV RF gun at 1.2 m in front of the accelerating section LAS of the CTF. The slanted line is the limitation due to the iris of the section, whose aperture depends on s. The positions of the RF gun, solenoid and section are sketched on top

accounting for the transverse motion with space charge along a drift ds is:

$$\begin{pmatrix} 1 & 0 \\ F_r/(\beta\gamma)\,\mathrm{d}s/(mc^2\beta) & 1 \end{pmatrix} \begin{pmatrix} 1 & \mathrm{d}s \\ 0 & 1 \end{pmatrix}$$

where F_r is the component of the radial force due to the space charge, divided by the radius. In the sub-matrix relative to the longitudinal motion, the element ds, figuring in the drift matrix is replaced by $\mathrm{d}s/\gamma^2$, and F_r by F_z, the longitudinal component of the force, divided by the longitudinal distance to the bunch centre. The formalism is three-dimensional allowing its use for elements without the rotational symmetry. In Figs. 7, 8, 9 the envelopes calculated from the analytical approximations are compared with the envelopes resulting from the matrix formalism, and the agreement between the two is good when theory predicts that the approximation is accurate.

8.1 Application to the Layout for CTF

Many elements of hardware and schemes imagined for the CERN Linear Collider [16] can be tested in the CLIC Test Facility (CTF). In CTF, it is expected that a 3-GHZ RF gun with a photocathode, associated with a pulsed synchrolaser will deliver charges higher than 6 nC in bunches shorter than 20 ps. The space-charge effect in RF guns has been studied by Kim [17]. Trains of these bunches will be used for loading a 30-GHZ transfer structure installed in the CTF [1],[18]. The dimensions of the bunches and the value of the energy correspond to a value of the parameter $a/(\gamma b)$ of the order of 1 or lower, for which the bunch lengthening due to the space charge is still acceptable for the application. On the contrary, the radial divergence due to the charge should be compensated by transverse focusing between the end of the gun and the end of the accelerating section, where the energy is raised at 40 MeV.

Figure 10 gives a preliminary solution for the optics for CTF: The initial energy is 3.9 MeV, the charge of 5.5 nC is distributed in an elliptical bunch. The initial length is 8.8 mm and the radius 6.4 mm. The maximum divergence is 63 mrad. For a uniform distribution of the charge, the r.m.s. values are obtained by dividing by $\sqrt{5}$ [2]. The envelope is represented from the exit of the RF gun, at $s = 0$, to the end of the 4.5 m, 10 MV/m, accelerating section. The beam is highly divergent at the gun exit: it is focused by a short solenoid into the iris of the accelerating section placed at a distance of about 0.8 m from the exit of the RF gun. The limitation due to the iris varies linearly with z, from 12.5 mm to 9 mm. The last iris is at the limit of the envelope. The section could be translated by 0.4 m towards the gun in order to have more clearance for the beam at the last iris, but the distance of 1.2 m in front of the section is necessary for the illumination of the photocathode of the gun by an off-axis mirror. The other envelope, diverging, is the one the focusing calculated for zero charge would give.

9 CONCLUSION

The scaling laws for the variation of the space-charge force with γ and with the aspect ratio a/b of the bunch have been derived from the approximations for the space-charge integrals. In the asymptotic domains of the variable $a/(\gamma\ b)$, the approximations give analytical solutions for the dynamics. Elsewhere, the approximations result in coupled transverse and longitudinal motions: a numerical solution has to be used. The solution well-known for the continuous beam represents a particular application of the solution for $\gamma \gg a/b$.

The envelopes obtained by the approximations have been compared with those resulting from the matrix solution. Though exact for the uniform distribution, the matrix solution does not give as much insight as the analytical investigation. Application of these methods has been made for the CLIC Test Facility.

ACKNOWLEDGEMENTS

I am indebted to Y. Baconnier for numerous discussions, and gratefully acknowledge K. Hübner for carefully reading the manuscript.

References

[1] Y. Baconnier, R. Bossart, K.H. Geissler, J.C. Godot, K. Hübner, H. Kugler, J.H.B. Madsen, A.J. Riche, G. Suberlucq
The CERN Linear Collider Facility
1990 Linac Conference, Los Alamos, NM.

[2] F.J. Sacherer
R.M.S. envelope equations with space charge
IEEE Trans. Nucl. Sci. **18**, 1105 (1971).

[3] K.L. Brown, D.C. Carey, C. Iselin, F. Rothacker
TRANSPORT, A Computer Program for Designing Charged Particle Beam Transport Systems
CERN 80-04 (1980).

[4] E. Keil
Beam Beam Interaction in p-p storage rings
International School of Particle Accelerators, CERN 77-13, p. 315.

[5] E. Durand
Electrostatique I (Masson, Paris, 1964) p. 338.

[6] J.R. Pierce
Theory and Design of electron beams (Van Nostrand, New York, 1950).

[7] Y. Baconnier, A. Pisent
CLIC Test Facility: The photocathode test bench
CLIC Note 104 (1989).

[8] E.A. Heighway and M.S. de Jong
TRANSOPTR, A Beam Transport Design Code with Space Charge, Automatic Internal Optimization and General Constraints
AECL 6975,
Accelerator Physics Branch, Chalk River Nuclear Laboratory.

[9] K.R. Crandall and D.P. Rusthoi
Documentation for TRACE: an interactive beam transport code
Los Alamos, January 1985.

[10] K.R Crandall and T.P. Wangler
PARMTEQ, A Beam Dynamics Code for the RFQ Linear Accelerator,
Workshop on Linear Accelerator and Beam Optics Codes, San Diego, 1988, AIP Conference Proceedings, Vol. 177 (1988), p. 22.

[11] I. Borchardt, E. Karantzoulis, H. Mais, G. Ripken
Calculation of Transverse and Longitudinal Space Charge Effects with the Framework of Fully Six-Dimensional Formalism
Desy 88-013, February 1988.

[12] M. Martini, O. Ponomarev
Modelling of space charge effects in the CERN Proton Synchrotron
IEEE 1991 Particle Accelerator Conference, San Francisco, 6-9 May 1991.

[13] B. Bru
GALOPR, a Beam Transport Program with space charge and bunching
3rd Int. Conf. on Charged Particle Optics, Toulouse, April 1990.

[14] P.M. Lapostolle,
Effets de la charge d'espace dans un accélérateur linéaire à protons
CERN internal report AR/Int. SG/65-15.

[15] P.M. Lapostolle,
Quelques propriétés essentielles des effets de charge d'espace dans les faisceaux continus
CERN internal report ISR-DI/71-6 (1971).

[16] W. Schnell
The study of a CERN Linear Collider
CERN-LEP-RF/88-48, and Linear Accelerator Conference, Williamsburg, Oct. 1988.

[17] K.J. Kim
RF and space-charge effects in laser-driven RF electrons guns
Nucl. Instrum. Methods **A275**, 201 (1989).

[18] K. Hübner
Generation of 30 GHZ RF power in the CLIC Test Facility
CERN/PS 91-06(LP) and CLIC Note 134.